ELSEVIER

Contents lists available at ScienceDirect

Geosystems and Geoenvironment

journal homepage: www.elsevier.com/locate/geogeo



Assessment of heavy metal contamination of sediments in popular tourist beaches of the Kerala State, southern India: Implications on textural and mineralogical affinities and mitigation

Mu. Ramkumar^a, R. Nagarajan^{b,c}, P. Athira^{a,*}, Anupam Sharma^d, P. Gopika^a, AL Fathima^a, G. Sugavanam^a, A. Manobalaji^b, R. Mohanraj^e

- ^a Department of Geology, Periyar University, Salem 636011, India
- ^b Department of Applied Sciences (Applied Geology), Curtin University Malaysia, Miri, Sarawak 98009, Malaysia
- ^c Curtin Malaysia Research Institute, Curtin University, Miri, Sarawak 98009, Malaysia
- ^d Birbal Sahni Institute of Palaeosciences, 53 University Road, Lucknow 226007, India
- ^e Department of Environmental Management, Bharathidasan University, Tiruchirappalli 620024, India

ARTICLE INFO

Article history: Received 28 March 2023 Revised 30 October 2023 Accepted 7 November 2023

Handling Editor: Bekun Festus Victor

Keywords: Bulk chemistry Beach sediments Total trace metals Pollution status Tourist beach Southern India

ABSTRACT

Beaches form one of the most contaminated sedimentary environments by a myriad variety of anthropogenic activities, including tourism and recreational activities. The concentrations of metals and their pollution levels were studied for four tropical tourist beaches in Kerala state, Southern India. Bulk geochemical and mineralogical analyses of 16 sediment samples were performed to determine the environmental status and the environmental risk level using various geochemical indices. Based on the enrichment of TiO2 and SiO2 concentrations, the samples were grouped into ilmenite-rich samples (IRS) and quartz-rich samples (QRS) respectively and the geochemical signatures are significantly different. Mineralogically, the IRS group is dominated by ilmenite, quartz, sillimanite, zircon and rutile while the QRS group consists of quartz, spinel and calcite and garnets are common in both groups of sediments. Despite the variation in the trends of pollution indices, it has been found that Kovalam beach sediments are enriched with W, Th and U where, IRS with enrichment of W, U and Th while QRS only enriched with W and Th and not U. The mineralogical affinity of W with secondary tungsten-bearing minerals has been documented by the XRD analysis and these metals are mainly controlled by the geogenic sourced minerals. However, in terms of ecological risk, Pb, As and Cu have a considerable to moderate risk in both groups of sediments. Overall, both group of sediments shows a moderate risk. Based on the biological effect assessment the elements of concern are Pb and Zn in IRS and possible effect by the Cr, Cu and As in IRS and only by Cu in QRS. Though the prevalence of geogenic and anthropogenic processes and influences of metal enrichments are documented by the study, their relative influences, mobility and bioavailability need to be systematically studied.

© 2023 The Authors. Published by Elsevier Ltd on behalf of Ocean University of China. This is an open access article under the CC BY license (http://creativecommons.org/licenses/by/4.0/)

1. Introduction

Beaches are crucial landforms on Earth's surface that function as a depositional platform for sediments to build up. Beaches act also as substrates, nutrient sources and feeding grounds for several organisms. Beaches are tourist hotspots and attract people from all around the world due to the proximity to water where a variety of recreational and adventurous water and shore-based activities occur. The beach sediments serve as a major reservoir of certain

* Corresponding author.

E-mail address: athiraammu0778@gmail.com (P. Athira).

metals for a short and long period of time – received by both continental and marine sources (Selvaraj et al., 2004; Long et al., 2006; Kumar et al., 2017; Moodley et al., 2021; Gunes, 2022) and thus ideal sites for the study of metals concentration and pollution levels. Any toxic chemical that contaminates coastal habitats including lakes and oceans, is referred to as beach pollution. It includes everything from oil and sewage to plastic, trash, and litter. Chemicals and debris are two common sources of beach contamination. All living things are harmed by this pollution, which also has negative economic and environmental effects. The higher the concentration, the more toxic the element. Even though Fe, Zn, Cu and Mg are vital metals because they play significant

functions in the biological system when there is an abundance of them, they get toxic. However, heavy metals that have relatively high density are highly poisonous even at low concentrations. Some heavy metals such as Fe, Co, Ni, Cr, Cd, Pb, Zn, Mn and Cu are regarded as serious pollutant metals in aquatic ecosystems due to their environmental perseverance, toxicity, and ability to incorporate into food chains (Rehab et al., 2022). It is also essential to determine geogenic and/or anthropogenic sources (Santos et al., 2004; Hossain et al., 2019; Anandkumar et al., 2022; Wang et al., 2023) of these metals with which effective remedial and/or mitigation measures can be designed and implemented. From an environmental standpoint, they are understanding how contaminated beaches could help in evaluating the qualities and trends of contaminants as well as, if people come in contact with sand, the consequences on public health (Francois et al., 2011). Investigating the distribution of heavy metals in surface sediments is useful for understanding the contamination in the marine environment (Wang et al., 2023). Sediment properties, metal characteristics, pH, organic matter, and redox potential are significant factors influencing the accretion and availability of heavy metals in sediments (Nagarajan et al., 2023). Studying beach pollution aids in reducing coastal pollution and developing marine protected areas also known as the 'National Parks of the Ocean', which can benefit human health and well-being while preserving vital ecosystems and seafood stocks (e.g., Djumanto et al., 2022; Hailu et al., 2023; Khuu et al., 2023). Thus, protecting the ecologically sensitive, aesthetically and economically important region from being polluted (especially from heavy metals) is a serious concern from the environmental perspective. The metals found in sediments (also soils) can become toxic if their specific threshold values are exceeded. The concentrations of metals along with their pollution level or toxicity status should be addressed for all the human-populated and rapidly urbanizing beaches to find the potential impacts of those metals due to their harmful nature to biological organisms. As bioaccumulation of those metals in sediments affects the metabolism of several species including fishes and crustaceans (Zhong et al., 2018; Gayathri et al., 2020; Anandkumar et al., 2020). From the primary consumer, the toxic metals enter all the way up to the humans in the food chain and may result in severe health risks (Isangedighi and David, 2019; Anandkumar et al., 2020). Therefore, to prevent the damage caused by heavy metals in the sand, it is necessary to investigate the harmful metal content of coastal sand and the degree of contamination. Metals are transported naturally from their source areas (Nagarajan et al., 2019) to beaches through stream runoffs and also by washouts at some point of heavy rainfall (Sheela et al., 2012). Other contributions are atmospheric fallouts and offshore sediments transported by waves and currents. But continuous stresses on beaches through anthropogenic activities inclusive of rapid urbanization, industrialization and tourism (Feng et al., 2004; Qiao et al., 2013; Bray et al., 2022; Nagarajan et al., 2023; Dessai, 2023) account for more mobile litters (which carries metals) and accumulated in beaches, which leads to elevating selective metal concentrations in soils and sediments eventually (Buzzi et al., 2022). Worldwide, many researchers have assessed beach sediments in terms of environmental monitoring (Anandkumar et al., 2022; Jéssica et al., 2021; Gowwyn-Paulson et al., 2022; Harmesa et al., 2023), coastal erosion and management (Garzon et al., 2022; Evelpidou et al., 2022; Saengsupavanich et al., 2023), coastal morphological changes (Dodge-Wan and Nagarajan, 2019; Anandkumar et al., 2019; Hossain et al., 2023; Irrgang et al., 2022), provenance (Nagarajan et al., 2019; Mohanty et al., 2023), economic potential (Gowwyn-Paulson et al., 2022; Hossain et al., 2023a; Mohanty et al., 2023) radiation hazards (Mahmoud et al., 2022; Abbasi et al., 2023) and microplastics (Ventakatramanan et al., 2022; Anshuman et al., 2023) etc. towards the development of sustainable tourism based the UN-SDGs. The study area has multiple unique factors, such as the famed tourist spot, tropical environment, coastal urban area, rough sea, high coastal erosion and sandy beaches with placer mineral accumulation. The exponential growth of coastal tourism in the tropical urban areas of Kerala in the last few decades has caused drastic environmental changes and thus had an impact on the local ecology (Ghosh and Datta, 2012). In this light, previous studies including Suresh et al. (2015), and Vineethkumar et al. (2020) attempted to document heavy metal accumulation in the beach sediments of coastal Kerala State, on a local scale and other areas such as microplastics (Kaviarasan et al., 2022) and coastal morphology monitoring system (Ramesh et al., 2023) also have been addressed. Recently, Rejith et al. (2021, 2022) characterized the detrital heavy minerals in terms of rare earth elements, crystal structure and morphology. Detailed research on the southern part of Karela with the reasons for the heavy metals is not addressed yet. Thus, in this work, we studied the concentration of metals along the four tourist beaches of Kerala State (near Kovalam, Thiruvananthapuram District; a famous tourist destination in the Kerala state) to documenting its pollution status, enrichment level and risk levels in line with sustainable ecotourism initiatives. This research is strategically important for the further development of eco-tourism in the study area.

2. Study area

The study area (Fig. 1) is located in the southern part of the state of Kerala (in the western boundary of Thiruvananthapuram District) in India surrounded by the Arabian Sea on the west and the Western Ghats on the east and bounded between the latitudes 8°21′29.21″ N and 8°26′22.82″ N; longitudes 76°57′27.69″ E and 77°10′44.34″ E. The tropical maritime climate and scenic natural beaches make this place an excellent spot for tourism and is very famous for its crescent-shaped sandy beaches, rocky cliffs and wavy waters. For the present study, four beaches were selected based on the coastal dynamics and the natural profiles of the beaches. Among these four study sites, the northernmost beach Pozhikkara (P) is located at the confluence of the Killi River and the region is surrounded by several tourist resorts. Hawa (H) and Lighthouse (L) beaches are located near the biggest tourist destination in this area — Kovalam Town, which is located in the

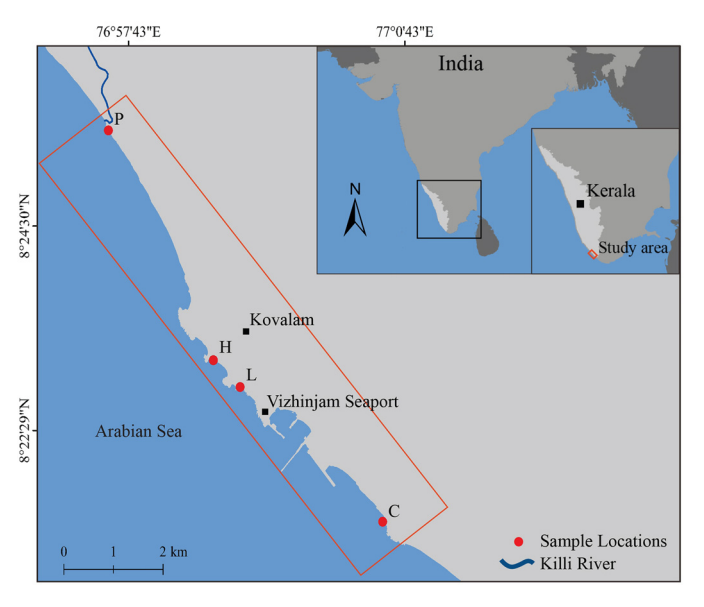


Fig. 1. Location map of the study area shows the sampling locations.

north of Vizhinjam port. The Chowara (C) Beach is located in the south of Vizhinjam port and is slightly away from the urban and tourist populations. All these beach stretches are under a microtidal regime (Pradeep et al., 2022).

3. Materials and methods

3.1. Sample collection

A total of 16 sediment samples from the surface of the four beaches covering the region from Berm/Hightide-subtidal region along a transect each: Pozhikkara (P): P1, P2, P3, P4; Hawa (H): H1, H2, H3, H4; Light House (L): L1, L2, L3; and Chowara (C): C1, C2, C3, C4, C5 were collected and the locations of these beaches are shown in Fig. 1. At each location, the samples were collected perpendicular to the shoreline from onshore to offshore, i.e., two samples respectively from berm/hightide water line to low tide waterline and one or two samples in between. Surface sediment samples were collected using uncontaminated plastic scoops and transferred to plastic zip-lock covers. Then the sample covers were labelled and taken to the laboratory and stored in the refrigerator at 4°C.

3.2. Sample processing

All the samples were thawed and allowed to reach ambient temperature before the sample processing. The sediment samples were washed with distilled water to remove sea salt followed by a drying treatment at 60°C in an air-oven. Approximately 100 g of sediment sub-samples were taken after homogenizing, coning and quartering. Then the samples were dry-sieved at $\frac{1}{2}$ intervals in a semi-automatic sieve-shaker and the weight of sediment fractions remaining in each of the sieves were measured, tabulated and graphical measures of mean size, standard deviation, skewness and kurtosis were computed following the procedures detailed in Ramkumar et al. (2000) and in this paper, only the mean size is utilized for want of brevity. Another fraction of the 30 g sediment sample was taken from the homogenized cone and quartered sample for powdering to <63 μ m using an agate mortar and pestle.

3.3. Bulk geochemistry

The powder was used for mineralogical, major, trace and REE analyses. The sediments were then analyzed for bulk geochemistry of oxides of ten major elements (Si, Al, Fe, Mn, Mg, Ca, Na, K, Ti and P) and the metals (Fe, Mn, Cu, Pb, Zn, Th, Nb, U, W) using ED- XRF and were measured in fused discs and analyzed in pressed pellets as per the method of Lozano and Bernal (2005) in a Siemens SRS 3000 wavelength dispersive X-ray fluorescence (XRF) spectrometer in the Birbal Sahni Institute of Palaeosciences, Lucknow, India. The precision of the analysis is <10% for both major and trace elements. With the help of the ICP-MS instrument, the concentrations of metals (Cr, Co, Ni, As, V and Ba) and REEs were measured.

3.4. Bulk mineralogy: XRD analysis

X-ray diffraction analysis was also carried out to identify the mineralogy of the samples. Using an agate mortar and pestle, sixteen samples from 4 locations were ground into a powder \leq 63 μ m, and the powders were then subjected to X-ray diffraction analysis for mineralogy. The Birbal Sahni Institute of Palaeosciences (BSIP) in Lucknow conducted the analyses. The samples were continually measured at 2θ angles with a step size of 0.01° between 3° and 80°. In order to determine the mineral species included in the

samples, the resulting diffractograms were analysed for peaks, patterns, and phases using Analytical B.V. highscore software, which is manufactured and licenced under B.V.

3.5. Statistical analysis

The quantitative data on the textural properties and the geochemical abundances were normalized and subjected to principal component analysis following Ramkumar et al. (2006) using SPSS software (version 17.0). Accordingly, varimax rotated factor scores are considered for the analysis. The factors that have more than eigenvalue of 1, explaining more than 5% of the data variance are considered for geological interpretations.

3.6. Environmental assessment

Various pollution and risk indices namely, contamination factor (CF), enrichment factor (EF), geo-accumulation index (Igeo) and pollution load index (PLI) and the risk indices namely, ecological risk factor (ER), potential ecological risk index (RI) and ERL and ERM were computed for enrichment/contamination status of the 15 selected metals. The mathematical formula of each index and their range and classification are summarised in the Supplementary Data, Table S1. These environmental indices are based on the normalization of particular elements against the background values to determine the enrichment of metals by natural and anthropogenic activities. The normalization is traditionally aimed at removing the effect of grain size and mineralogy on the observed compositional variations in the data (Ho et al., 2012). The contamination factor (CF) is one of the critical indices of pollutant assessment that is used to estimate metal contamination level in the sediments according to its baseline value (Hakanson, 1980). For the baseline value, the Upper Continental Crust (UCC) value proposed by McLennan (2001) was used for those individual metals. Contamination levels for metals are categorized as per Harikumar and Jisha (2010) and Kumar et al. (2017).

The enrichment factor (EF) was calculated to evaluate the enrichment of metal by computing the ratio of metal's concentration normalized with Fe or Al to the baseline value of metal normalized by the baseline value of Fe or Al (McLennan, 2001). In this study, Al was considered as a baseline value due to its conservative nature, immobility and its abundance in sediments and soils (Chen et al., 2007). The EF values are classified according to the study of Kumar et al. (2017) and the enrichment categories are presented in Supplementary Data, Table S1. If the EF values are close to unity for the given metal represents that those metals are likely to be derived from the crustal materials from the source areas. Similarly high EF values can be related to either natural or anthropogenic (Zoller et al., 1974).

The geo-accumulation index (I_{geo}) (Müller, 1969) was used for measuring or assessing the level of metal pollution in the sediments. For calculating I_{geo} values, the baseline values of the Upper Continental Crust (UCC) of McLennan (2001) were used and the I_{geo} was classified into seven classes (Müller, 1981; Buccolieri et al., 2006; Kumar et al., 2017) as listed in Table S1. The Pollution Load Index (PLI) was used to calculate the mutual contamination effect in the sediments (Tomlinson et al., 1980) based on the CF values of each metal and the level of pollution was classified based on Angulo (1996) as presented in Supplementary Data, Table S1.

Ecological risk factor (ER) is calculated to identify the potential ecological risk for the five metals [number denotes its toxic-response factor] (As[10], Cr[2], Pb[5], Cu[5], Zn[1]) (Hakanson, 1980). The five risk categories as per Mugoša et al. (2016) are listed in Supplementary Data, Table S1. The potential ecological risk index (RI) is defined as a sum of ecological risk factors of all metals (Hakanson, 1980) and the

category of level of risk (Mugoša et al., 2016) and is listed in Supplementary Data, Table S1. The Effects Range-Low (ERL) and Effects Range-Median (ERM) are the two guideline values proposed by Long et al. (1995) for contamination of biological systems of natural environments by six metals namely, As, Cr, Co, Pb, Zn and Ni. The levels have been classified into 3 categories: (1) below ERL: minimal-effect range or effects rarely observed, (2) ERL to ERM: possible-effect range, and (3) above ERM: maximal-effect range. When the concentration of the selected metals is elevated in sediments, they become toxic and may have chronic effects on living organisms (Long et al., 1995; Jayaprakash et al., 2012). These ERL and ERM values are related to the potential impact on the biota and were derived from multivariate analyses of the relationships between metal levels in sediment and benthic community health in a variety of environments. The values recorded below ERL values do not have any adverse effect and values exceeding the ERM values may have adverse effects and be of ecological concern (Long et al., 1995).

4. Results

Based on the weight percent of two major oxides, SiO₂ and TiO₂ the sediment samples were separated into two groups as IRS (ilmenite-rich samples; *n*: 10): P2, P3, P4, H1, H2, H3, H4, L1, L2. L3 and QRS (quartz-rich samples; n: 6): P1, C1, C2, C3, C4, C5 (Table 1). The ilmenite-rich samples (IRS) of samples consist of fine, medium and coarse sands that account for 60%, 30% and 10% respectively. The quartz-rich samples (QRS) are dominated by coarse sand (66.66%) whereas cobble and medium sands account for 16.66% and 16.66%, respectively. Distributions of IRS and QRS according to the locations and beaches have revealed that the locations P (except the sample P1), H, and L are grouped into ilmeniterich samples (IRS; n = 10), where the observed TiO_2 percentage is in a considerable amount and also have low SiO2 contents. Location C and the sample P1 from location P are depleted in TiO₂ (less than 7 wt.%) and are enriched with SiO₂ (>80%) and grouped into quartz-rich samples (QRS; n = 6). Among all the oxides, except SiO₂ and TiO₂, only Fe₂O₃ shows major variations between these two groups. Additionally, Fe₂O₃ is enriched in the IRS.

In the IRS, the metal's concentration is in the decreasing order of Fe > Th > Mn > Nb > W > Zn > Pb > Cr > U > Cu > V > Co > Ba > Ni > As. Whereas, in the QRS, it is: Fe > W > Mn > Cu > Pb > Th > Nb > Zn > Co > Cr > Ba > V > Ni > As (U is totally absent). In both groups, Fe is most abundant, and As is scarce. After Fe, W is most abundant in the QRS. In the IRS, Th is the second most abundant metal. Cu shows comparatively more abundance in QRS than in IRS (Table 1).

The XRD analysis results are summarised in Table 2. The IR samples consist mainly of quartz, ilmenite, sillimanite, zircon, rutile and xenotime and traces of pyrite, pseudobrookite, ferric arsenate and ulvospinel while QR samples mainly consist of quartz, spinel, and calcite and traces of epsomite. Garnet and pyroxene are common in both sample groups except few samples. Other minerals such as amphibole, monazite and scheelite were noticed in few samples of both groups.

The average CF values in IRS are in the decreasing order of W > Th > Nb > U > Pb > Cu > As > Zn > Fe > Mn > Co > Cr > V > Ni > Ba (Fig. 2a). For QRS (Fig. 2b), the average CF values are in decreasing order for the selected metals as W > Cu > Th > Nb > Pb > Co > As > Zn > Fe > Cr > Mn > Ni > V > Ba > U. This order is to a certain extent different from the IRS due to the less influence of sorting.

The calculated I_{geo} values vary significantly between the samples of IRS and QRS as presented in Fig. 3. In the IRS (Fig. 3a) the average I_{geo} values are in decreasing order of W>U>Th>Nb>Pb>Zn>As>Fe>Cu>Mn>Co>Cr>

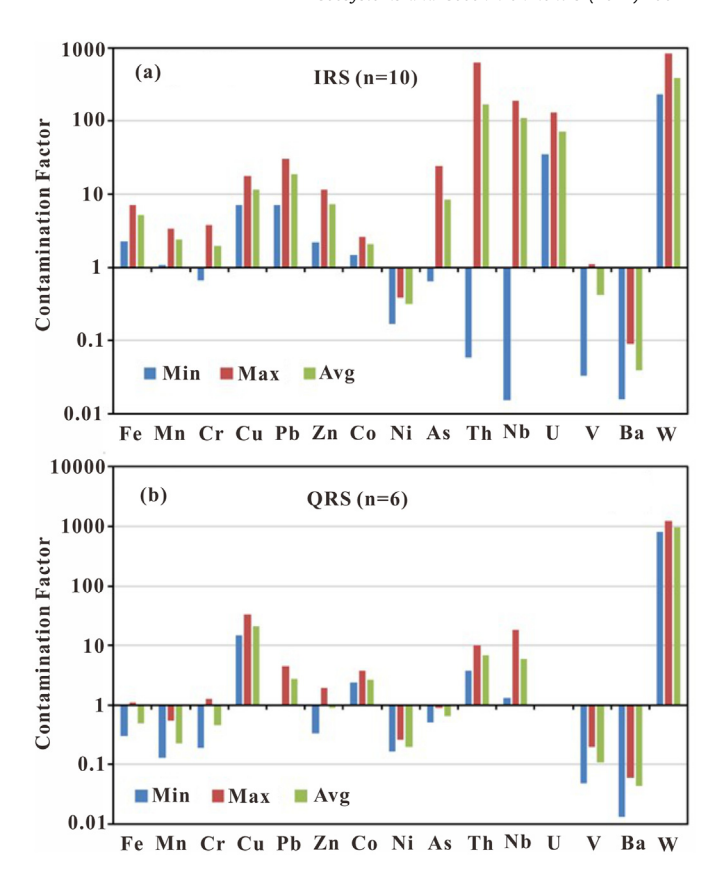


Fig. 2. Level of CF values for the Kovalam beach sediments (a) CF for IRS, (b) CF for ORS.

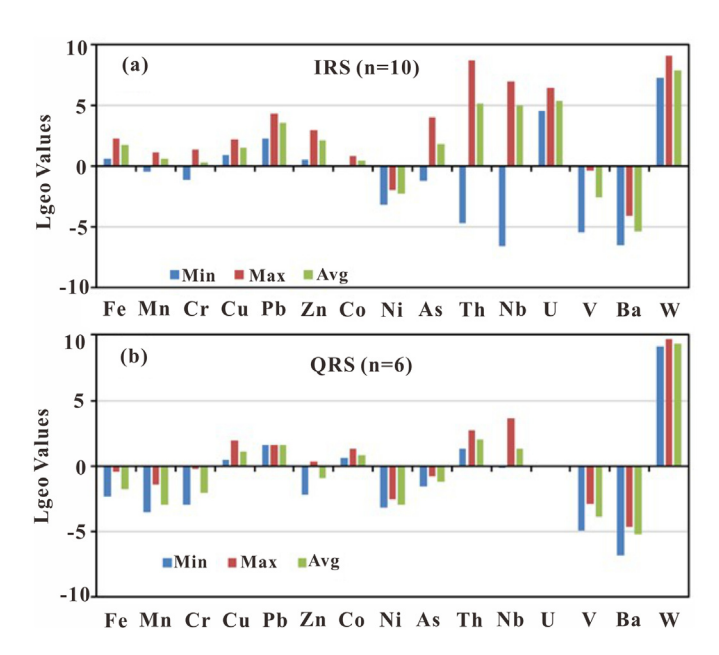


Fig. 3. Level of I_{geo} values for the Kovalam beach sediments (a) I_{geo} for IRS, (b) I_{geo} for QRS.

Ni > V > Ba. This order of contamination levels of metals is different from that of CF and the influence of mineralogical composition appears to have exercised control over this difference. Igeo values for QRS sediments (Fig. 3b) are in the ranges of -5.24 (Ba) to 9.33 (W) and their average values in the decreasing order are: W > Th > Pb > Nb > Cu > Co > Zn > As > Fe > Cr > Mn = Ni >

Geosystems and Geoenvironment 3 (2024) 100244

 Table 1

 Bulk geochemical results of Kovalam beach sediments.

meters	P-2														Quartz	rich samp	105 (Q10)	(– 0)						
		P-3	P-4	H-1	H-2	H-3	H-4	L-1	L-2	L-3	Min	Max	Avg	St.Dev	P-1	C-1	C-2	C-3	C-4	C-5	Min	Max	Avg	St.Dev
SiO ₂	17.07	68.24	32.02	33.13	10.27	35.21	46.84	6.10	15.25	10.10	6.10	68.24	27.42	19.61	83.85	86.54	86.58	90.51	86.00	87.95	83.85	90.51	86.91	2.21
Al_2O_3	5.76	4.85	5.78	8.05	4.42	7.10	6.69	3.74	7.30	3.92	3.74	8.05	5.76	1.50	2.69	2.02	3.09	1.74	2.53	3.12	1.74	3.12	2.53	0.56
Fe_2O_3	28.16	10.22	22.50	20.81	27.47	18.97	15.72	32.20	27.08	28.01	10.22	32.20	23.11	6.75	5.02	1.64	1.81	1.35	1.73	1.54	1.35	5.02	2.18	1.40
CaO	0.17	0.27	0.20	0.36	0.26	0.37	0.18	0.25	0.23	0.25	0.17	0.37	0.25	0.07	0.31	3.25	2.51	2.27	3.63	2.44	0.31	3.63	2.40	1.15
MgO	0.60	0.31	0.51	0.68	0.63	0.54	0.37	0.97	0.82	0.70	0.31	0.97	0.61	0.20	0.30	0.31	0.34	0.21	0.24	0.21	0.21	0.34	0.27	0.06
Na_2O	0.22	0.11	0.07	0.81	0.53	0.22	0.11	0.65	0.44	0.15	0.07	0.81	0.33	0.26	0.41	0.62	0.63	0.31	0.20	0.26	0.20	0.63	0.41	0.19
K_2O	0.03	0.04	0.02	0.04	0.03	0.05	0.06	0.02	0.03	0.03	0.02	0.06	0.03	0.01	0.07	0.34	0.22	0.24	0.30	0.31	0.07	0.34	0.25	0.10
MnO	0.24	0.08	0.19	0.17	0.20	0.15	0.13	0.26	0.22	0.22	0.08	0.26	0.19	0.05	0.04	0.02	0.01	0.01	0.01	0.01	0.01	0.04	0.02	0.01
TiO ₂	42.43	13.78	31.82	31.35	40.82	28.18	23.35	49.38	41.96	42.05	13.78	49.38	34.51	10.79	6.03	0.56	0.85	0.31	1.39	0.92	0.31	6.03	1.68	2.16
P_2O_5	0.13	0.05	0.27	0.11	0.74	0.43	0.30	0.18	0.23	0.79	0.05	0.79	0.32	0.26	0.04	0.03	0.03	0.03	0.04	0.10	0.03	0.10	0.05	0.03
Cr	131.0	55.6	208.6	160.7	211.0	315.5	156.8	116.9	121.3	158.3	55.6	315.5	163.5	70.0	37.2	18.3	27.8	16.0	25.8	106.3	16.0	106.3	38.6	34.0
Ni	15.4	7.4	15.7	12.7	13.5	14.4	13.4	16.8	13.9	15.9	7.4	16.8	13.9	2.6	11.5	8.0	8.6	7.3	7.3	9.8	7.3	11.5	8.8	1.6
Zn	729.7	155.8	253.3	527.5	658.1	520.2	309.6	811.6	587.0	654.0	155.8	811.6	520.7	215.7	137.8	55.5	61.8	36.7	23.9	67.4	23.9	137.8	63.9	39.7
Ga	113.0	18.4		83.8		54.4	43.6	106.1	86.3		18.4	113.0	72.2	34.6	BDL	BDL	BDL	BDL	BDL	BDL	-	-	-	-
Sr	18.0	5.5	12.6	16.4	12.7	14.5	7.4	20.4	15.7	14.1	5.5	20.4	13.7	4.5	4.5	55.2	39.5	35.0	54.9	38.1	4.5	55.2	37.9	18.5
Y	112.1	23.7	229.5	93.5	608.1	332.6	208.8	163.6	162.7	513.4	23.7	608.1	244.8	187.4	18.3	8.7	BDL	BDL	BDL	5.7	5.7	18.3	10.9	6.6
Zr	2579.0	6060.0	3942.0	1699.0	9170.0	4985.0	3440.0	3402.0	3671.0	8662.0	1699.0	9170.0	4761.0	2494.0	2670.0	358.7	286.3	222.2	686.4	462.1	222.2	2670.0	781.0	939.6
Nb	1910.0	552.7	1390.0	1340.0	1890.0	1240.0	975.6	2250.0	1840.0	0.2	0.2	2250.0	1338.8	688.5	223.3	15.9	27.8	BDL	52.2	33.4	15.9	223.3	70.5	86.4
V	12.0	14.8	52.6	3.5	76.9	119.9	107.1	18.0	13.7	28.7	3.5	119.9	44.7	42.5	21.3	7.5	11.7	5.2	13.3	11.4	5.2	21.3	11.7	5.6
As	4.6	1.0	15.3	2.4	13.9	23.7	15.7	5.4	7.0	36.0	1.0	36.0	12.5	10.9	0.8	0.9	1.0	0.8	1.3	1.0	0.8	1.3	1.0	0.2
Ba	24.7	8.7	16.3	18.5	19.4	20.2	19.6	48.9	20.4	17.8	8.7	48.9	21.5	10.5	7.2	33.4	22.9	22.1	28.6	31.1	7.2	33.4	24.2	9.4
Hf	582.7	87.5	780.4	783.2	2350.0	1010.0	892.8	902.1	894.2	0.2	0.2	2350.0	828.3	637.9	BDL	BDL	BDL	BDL	BDL	BDL	-	-	-	-
W	667.4	1670.0	713.7	947.8	484.4	916.4	1020.0	465.1	517.0	458.3	458.3	1670.0	786.0	376.0	2500.0	2210.0	1720.0	1780.0	1880.0	1640.0	1640.0	2500.0	1955.0	332.5
Pb	257.6	120.9	363.6	302.3	331.2	215.8	245.3	387.0	409.8	517.2	120.9	517.2	315.1	112.3	76.1	BDL	BDL	BDL	BDL	BDL	76.1	76.1	76.1	
Th	774.5	113.2	2470.0	405.5	6660.0	3390.0	2100.0	849.0	1370.0	0.6	0.6	6660.0	1813.3	2023.6	107.3	BDL	BDL	BDL	40.0	BDL	40.0	107.3	73.7	47.6
U	BDL	BDL	153.3	BDL	362.5	177.3	106.3	BDL	98.5	318.1	98.5	362.5	202.7	111.4	BDL	BDL	BDL	BDL	BDL	BDL	-	-	-	-
Cu	159.0	71.6	168.0	92.9	85.7	85.3	BDL	BDL	138.5	BDL	71.6	168.0	114.4	39.6	146.8	68.5	87.5	52.9	BDL	75.3	52.9	146.8	86.2	36.1
Co	43.6	28.5	25.1	37.3	39.3	44.3	36.2	33.4	32.8	34.6	6.1	68.2	27.4	19.6	40.0	63.3	44.2	45.0	40.5	40.6	40.0	63.3	45.6	8.9

Table 2XRD results of Kovalam beach sediments (IRS – ilmenite-rich samples and QRS – quartz-rich samples).

Mineral/Sample Number	IRS (n	= 10)									ORS (n = 6)				
rumber											- —	– 0)				
	P2	Р3	P4	H1	H2	Н3	H4	L1	L2	L3	P1	C1	C2	C3	C4	C5
Quartz	Х	X	X	X	X	X	X	Х	Х	Х	Х	Х	Х	X	X	X
Ilmenite	X	X	X	X	X	X	X	X	X	X	X					
Sillimanite	X	X	X	X	X	X	X	X	X	X	X					
Zircon			X		X	X	X	X	X	X						
Garnet group						X	X	X	X	X		X	X	X		X
Pyroxene group		X		X		X	X				X	X	X	X		
Spinel			X									X	X		X	
Rutile/Anatase	X			X	X			X	X	X						
Calcite/Aragonite								X					X	X	X	X
Amphibole group								X		X		X				
Monazite					X							X	X			
Xenotime	X				X					X						
Scheelite				X												X
Epsomite															X	
Pseudobrookite						X										
Magnesio									X							
chloritoid																
Pyrite										X						
Ferric arsenate		X														
Ulvospinel			Χ													

X indicates presence.

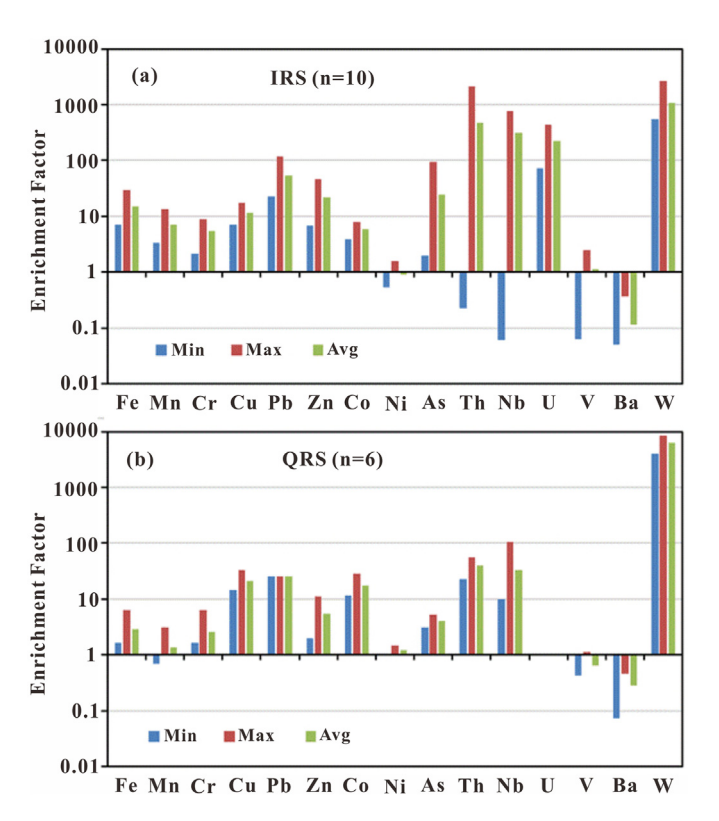


Fig. 4. Level of EF values for the Kovalam beach sediments for (a) EF for IRS, (b) EF for QRS.

 $V > Ba \ and \ U$ are recorded below the detection limit (BDL) for all the samples.

The enrichment factor values for both IRS and QRS groups are presented in Fig. 4a and b respectively. The calculated EF values (average) in the order of W > Th > Nb > U > Pb > As > Zn > Fe > Cu > Mn > Co > Cr > V > Ni > Ba for IRS and W > Th > Nb > Pb > Cu > Cr > Co > Zn > As > Fe > Cr > Mn > Ni > V > Ba for QRS respectively. Similarly, Ecological risk factor (ER) values in IRS and QRS were in the order of

Pb > As > Cu > Zn > Cr and Cu > Pb > As > Cr > Zn respectively.

5. Discussion

5.1. Mineralogical affinities of elements and geochemical mechanisms as revealed by statistical analysis

From total of 89.1% variance in IRS, explaining about 44.4% variance (Table 3) by positive loadings of P₂O₅, Y, Zr, As, U and REEs, and negative loading of Ga in the first factor suggests heavy mineral hosted nature of the heavy metals. This inference is further ascertained by mineralogical analyses (Table 2). In addition, affinities of REEs in more than one heavy mineral such as zircon, monazite and xenotime etc., and enrichment of HREEs in zircon are inferred. As zircon is highly resistant to weathering, its nature to host a large portion of the HREEs in its lattice positions (Aide and Aide, 2012) and enrichment of zircon is the major controlling factor of these metals in the sediments. Factor 2 with 25.8% of the variance is positively loaded by Fe, Mg, Mn Ti, Ni, Zn, Sr, Ba, Nb and Pb and negatively loaded by Si. K and W. The Fe-Mn oxides control the behaviours/abundances/enrichments-depletions of many metals. Affinity to heavy minerals such as rutile, and ilmenite and their control on Ti in these sediments is reaffirmed. The positive loading of Fe and Ti can be represented by the ilmenite, rutile, anatase and pseudo brookite in the sediments, which has been further confirmed by the XRD analysis. SiO₂, K₂O and W are negatively loaded in this factor, which may be due to the density difference between the Ti-bearing heavy minerals and W-bearing minerals in the sediments. The tungsten in these sediments is controlled by the presence of scheelite and other secondary mineral sources. Only 2 samples have recorded scheelite in the XRD analysis. Amongst naturally occurring W-minerals, scheelite minerals are recorded in two samples by XRD analysis. The absence of scheelite in other samples though they are enriched in W metal, may be due to the alteration of primary W mineral (i.e., Scheelite) can form many secondary tungsten minerals. The strong positive loadings of W with other rare earth elements and selected metals (Zn, Ni, V, Pb, Fe and Mn) may support this inference. Factor 3 explaining 6.7% of variance is positively loaded by the Nb, Hf and Th, which suggests the presence of Th-bearing minerals that control the Nb and Hf in addition

 Table 3

 Rotated component matrix components for ilmenite-rich samples (IRS) of Kovalam Beach.

Parameter	Rotated Principal Components													
	1	2	3	4	5	6	7							
SiO ₂	-0.360	-0.919	-0.084	0.060	-0.114	0.010	0.026	0.999						
Al_2O_3	-0.403	-0.207	-0.012	0.469	0.238	0.336	-0.505	0.850						
Fe_2O_3	0.226	0.958	0.086	-0.123	0.055	-0.072	-0.011	1.000						
CaO	0.075	-0.164	-0.002	0.180	0.138	0.907	0.001	0.907						
MgO	-0.008	0.912	0.017	-0.142	0.059	0.294	0.139	0.962						
Na ₂ O	-0.155	0.473	0.338	-0.222	0.197	0.694	0.088	0.940						
K ₂ O	-0.090	-0.624	-0.131	0.518	0.428	0.129	0.258	0.950						
MnO	0.121	0.971	0.039	-0.083	0.048	-0.169	-0.046	0.998						
ΓiO ₂	0.199	0.962	0.078	-0.120	0.104	-0.052	0.007	0.999						
P ₂ O ₅	0.979	0.132	-0.076	0.088	0.057	-0.012	0.081	0.999						
Cr	0.452	0.040	0.194	0.791	-0.007	0.224	-0.206	0.961						
Ni	0.187	0.850	-0.062	0.428	-0.083	-0.193	0.039	0.990						
Zn	0.173	0.844	0.095	-0.090	0.446	0.089	0.107	0.978						
Ga	-0.716	0.489	0.090	0.054	0.479	0.069	0.011	0.998						
Sr	-0.151	0.923	0.036	0.080	0.151	0.217	-0.087	0.961						
Y	0.972	0.167	0.103	0.111	0.030	0.012	0.053	1.000						
Zr	0.890	-0.180	-0.012	-0.299	-0.046	-0.043	0.145	0.940						
Nb	-0.326	0.562	0.744	0.024	0.061	-0.004	-0.114	0.993						
V	0.417	-0.353	0.303	0.739	0.071	-0.133	0.176	0.990						
As	0.756	0.060	-0.460	0.427	-0.038	-0.102	0.112	0.994						
Ba	-0.253	0.751	0.242	0.079	0.049	-0.013	0.541	0.988						
Hf	0.383	0.146	0.866	0.125	0.082	0.145	-0.071	0.967						
W	-0.403	-0.887	-0.073	-0.089	-0.010	0.080	0.065	0.974						
Pb	0.428	0.741	-0.344	-0.082	-0.220	0.039	0.017	0.907						
Th	0.585	-0.068	0.758	0.241	-0.220 -0.017	0.009	-0.123	0.996						
U	0.985	0.026	0.029	0.103	-0.068	-0.023	-0.123	0.991						
Cu	-0.230	0.057	0.236	-0.003	-0.168	-0.023	-0.910	0.975						
Co	0.155	0.151	0.185	0.344	0.841	0.071	-0.089	0.920						
La	0.133 0.991	0.073	0.083	0.070	0.000	-0.020	0.010	1.000						
Ce	0.992	0.073	0.063	0.056	0.010	-0.020 -0.017	0.017	0.999						
Nd	0.994	0.082	0.003	0.032	0.014	-0.017 -0.018	0.017	0.999						
Sm	0.994	0.082	0.047	0.032	0.006	-0.018 -0.020	0.028	1.000						
Eu	0.984	0.082	0.047	0.072	0.025	-0.020 -0.009	0.021	0.999						
Gd	0.993	0.088	0.048	0.069	0.025	-0.009 -0.021	0.027	1.000						
Gu Dy	0.990	0.108	0.028	0.069	0.016	-0.021 -0.009	0.023	1.000						
Ho	0.990 0.987	0.108	0.035	0.069	0.016	-0.009 0.002	0.027	0.999						
Er Saar	0.978	0.184	0.056	0.057	0.040	0.017	0.030	0.999						
Γm	0.949	0.282	0.087	0.072	0.050	0.044	0.032	0.999						
Lu	0.893	0.404	0.134	0.068	0.079	0.073	0.055	0.998						
ΣREE	0.993	0.081	0.057	0.055	0.008	-0.018	0.018	0.999						
Mz	0.011	0.276	-0.065	-0.222	0.851	0.212	0.233	0.954						
Eigen value	18.222	10.598	2.742	2.615	2.340	1.831	1.722							
Variance%	44.4	25.8	6.7	6.4	5.7	4.5	4.2							

Significant loadings a e shown in bold and italics letter.

to rutile and zircon respectively, that are the main hosts for Nb and Hf. Factor 4 explains 6.4% of the total variance and has moderate positive loadings of Cr and V and weak positive loading by K. These metals would have been controlled by the chromian spinels or garnets. Garnets from the west coasts of India are rich in Fe and belong to the almandine group, which contributes up to 1094 ppm of total REEs and also hosts some minor elements such as Zr, Zn, Th, Ba, V and Cr, etc. (Rejith et al., 2022). Yet, sillimanite mineral grains from beaches in the study area mainly consist of Al₂O₃ and SiO₂ followed by other elements such as P, Ca, and Fe. In addition, REEs are recorded up to 222 ppm and other trace metals such as Zr, V, Cr, Zn and Ga are also recorded for their high abundance. Thus, Cr and V in these sediments are associated and controlled by the sillimanites and garnets and the presence of these minerals is confirmed by XRD analysis. Factor 5 represents 5.7% of the total variance and is explained by the positive loading of Co and mean grain size indicates that Co is adsorbed in the fine sediments.

Factor analysis of QRS sediments (Table 4) shows the influences of 5 factors explaining a total variance of 100%. The first factor with positive loadings of Fe, Mn, Ti and other trace elements except Sr, Cr, As, Cu, Co and Eu accounts for 51% of the total variance. Though the REEs and trace metals are mainly controlled by the heavy minerals such as zircon, ilmenite, rutile, garnet and monazite in the

QRS, their concentrations are lesser compared to IRS. These sediments are enriched in quartz and are related to the mean grain size of the samples. The light fraction of minerals is mainly represented by quartz and feldspar but feldspars are not obvious in the XRD analysis. The association of light minerals has been confirmed by the negative loading of Si, K and Ba together with mean grain size in this factor. Tungsten is also loaded together with other metals and is mainly controlled by the primary and secondary Wbearing minerals as discussed above. Factor 2 is represented by the positive loadings of Fe, Mn, Ti oxides and other trace metals such as Ni, Zn, Y, Zr, Pb and Cu and explains 23.2% of the total variance. Some of the metals are loaded in this fraction in addition to the first factor indicating that in addition to heavy minerals, these metals are controlled by the Fe-Mn oxides coated in the finer fraction of the sediments. A strong negative loading of Ca, K, Sr, As, Ba, Eu and mean grain size indicates that the grain size variation and the presence of carbonate minerals and pyroxenes control these metals. Eu alone is loaded in this factor, which can be due to the substitution of Eu for Ca or Sr in carbonates. Factor 3 explains 10.5% of the total variance and is represented by the positive loadings of Al, P, Cr, and Ni, which can be related to the presence of Cr-spinels and/or garnets. The garnet species dominated in the Kovalam Beach is almandine, which belongs to the pyralspite

Table 4Rotated component matrix components for quartz-rich samples (QRS) of Kovalam Beach.

Parameter	Rotated Prin	Communalities						
	1	2	3	4	5			
SiO ₂	-0.853	0.026	-0.044	-0.518	0.033	1.000		
Al_2O_3	0.214	-0.039	0.693	0.397	-0.561	1.000		
Fe ₂ O ₃	0.800	0.577	-0.028	0.158	-0.027	1.000		
CaO	-0.424	-0.895	-0.107	-0.016	0.089	1.000		
MgO	0.132	0.133	-0.250	0.950	0.008	1.000		
Na ₂ O	-0.248	0.194	-0.187	0.893	0.262	1.000		
K ₂ O	-0.513	-0.768	0.167	-0.094	0.332	1.000		
MnO	0.795	0.566	0.010	0.140	0.167	1.000		
TiO ₂	0.850	0.517	0.012	0.080	-0.068	1.000		
P_2O_5	0.064	-0.037	0.962	-0.260	-0.034	1.000		
Cr	0.014	0.020	0.978	-0.191	-0.077	1.000		
Ni	0.567	0.607	0.515	0.211	-0.014	1.000		
Zn	0.582	0.710	0.260	0.291	0.079	1.000		
Sr	-0.439	-0.873	-0.102	0.045	0.179	1.000		
Y	0.688	0.509	0.202	0.177	0.442	1.000		
Zr	0.865	0.501	0.005	0.033	-0.014	1.000		
Nb	0.867	0.483	0.038	0.089	-0.078	1.000		
V	0.876	0.258	0.189	0.197	-0.302	1.000		
As	0.176	-0.889	0.071	-0.042	-0.414	1.000		
Ba	-0.511	-0.765	0.240	-0.021	0.310	1.000		
W	0.728	0.334	-0.294	0.223	0.471	1.000		
Pb	0.770	0.634	-0.029	0.073	0.014	1.000		
Th	0.921	0.350	-0.127	-0.038	-0.108	1.000		
Cu	0.286	0.829	0.239	0.405	0.103	1.000		
Co	-0.299	-0.195	-0.252	0.392	0.809	1.000		
La	0.980	0.153	0.073	-0.087	-0.051	1.000		
Ce	0.981	0.148	0.071	-0.094	-0.052	1.000		
Nd	0.982	0.145	0.064	-0.092	-0.051	1.000		
Sm	0.985	0.130	0.045	-0.085	-0.068	1.000		
Eu	0.308	-0.802	0.496	0.103	0.066	1.000		
Gd	0.971	0.189	0.105	-0.075	-0.065	1.000		
Dy	0.954	0.181	0.148	0.105	-0.154	1.000		
Ho	0.873	0.149	0.362	0.207	-0.202	1.000		
Er	0.797	0.044	0.366	0.457	-0.139	1.000		
Tm	0.838	0.166	0.273	0.443	0.002	1.000		
Lu	0.758	-0.049	0.363	0.539	-0.003	1.000		
Σ REE	0.981	0.148	0.071	-0.090	-0.053	1.000		
Mz	-0.775	-0.621	0.034	-0.002	-0.112	1.000		
Eigen value	19.362	8.808	3.984	3.684	2.162			
Variance%	51.0	23.2	10.5	9.7	5.7			

Significant loadings a e shown in bold and italics letter.

group (Rejith et al., 2022) where transition metals present in two coordinated positions such as Mn²⁺ in triangular dodecahedra of 8-coordinated positions whiles Fe³⁺ and Ti⁴⁺ are octahedral coordinated positions (Rejith et al., 2022). Mg, Na and Lu are positively loaded and Si is negatively loaded in factor 4 and explains 9.7% of the total variance. The association of these metals can be related to the presence of either dolomites or sheet silicate minerals such as amphiboles and pyroxenes. Na can be closely concentrated in dolomites due to diagenetic effects depending on the salinity of dolomitizing fluids (Rahimi et al., 2016; Hui et al., 2022). Factor 5 explains 5.7% of the total variance and is represented by the negative loading of Al and positive loading Co, which indicates that Co is not controlled by the carbonate and Fe-Mn oxides and may be controlled by the organic fractions of the sediments.

5.2. Assessment of heavy metal contamination

Based on the average CF values, many metals namely, Cu, Pb, Zn, As, Th, Nb, U and W are classified under the very high contamination category; Mn, Cr, and Co belong to the moderate contamination category; Ni, V, and Ba are considered under the low contamination category; and only Fe is classified under considerable contamination category respectively for the ilmenite rich samples. In the case of quartz-rich samples, Cu, Th and W show very high contamination; Pb and Co belong to the moderate contamina-

tion category; Fe, Mn, Cr, Zn, Ni, As, V, and Ba are under the low contamination category; only Nb is considered under considerable contamination category. In both the groups (IRS and QRS), W is the most contaminated metal regardless of variations in mineralogy. According to the I_{geo} values of the studied metals in the IRS, 25.9% of metals (i.e., mostly Ni, V, and Ba) have not contaminated the sediments. Mn, Cr and Co are mainly in the ranges of unpolluted to moderately polluted category, which represents 18.2%. Zn, Cu and As are mainly in the ranges of moderately polluted (Igeo value of 1-2) to moderately polluted to severely polluted (Igeo value of 2-3) category, which represents 25.2% of the overall metals. Pb falls into the severely polluted (Igeo value of 3-4) to severe to extremely polluted category (Igeo value of 4-5) and represents 18.9% in total. Th, Nb, W, and U have recorded very high Igeo values and thus are categorized as extremely polluted ($I_{geo} > 5$) category, which represents 19.6%. When compared with IRS, QRS are not polluted by Fe, Mn, Cr, Zn, Ni, As, V and Ba and are categorized as unpolluted (avg: Igeo < 0). Other metals such as Co, Cu, Pb, Th and Nb fall into the moderate to severely polluted category and only W is recorded in the extremely polluted category and the Igeo values of W are recorded higher in QRS than that of in IRS.

Based on the EF values, IRS is very severely enriched with W, U, Nb, Th and Pb; severely enriched with Fe, Zn and As; moderately to severely enriched with Mn, Cr, and Co; and U shows a minor enrichment and has U contents below the detection limit in few

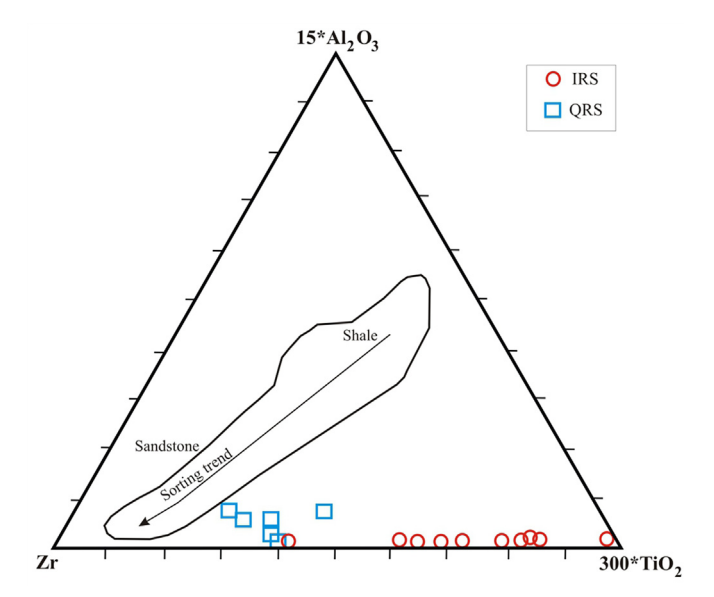


Fig. 5. Al₂O₃-TiO₂-Zr plot shows the effect of sorting (after Garcia et al., 1994).

samples. Only Ba and Ni in these sediments did not show any enrichment. In the case of QRS, the trend is very different except for W, Th, Nb and Pb, which are very severely enriched; Cu and Co are severely enriched. However, 5 and 4 samples contain Pb and Th below the detection limits respectively. A moderate to severe enrichment of Zn; moderate enrichments of As, Fe, Mn and Cr; and minor enrichment of Ni are observed. V, Ba, and U (BDL) did not show any enrichment. Though there is a similarity in the enrichment of metals between the sediments, the level of enrichment is much lower in QRS compared to IRS. Besides, W is enriched much higher in QRS than in the IRS.

In general, EF values less than 10 can be considered crustal/natural origin due to the differences in the composition of local sediments and reference sediments used for EF calculation (Pekey, 2006). In addition, the sediments of beach environments are continuously subjected to wave and surf action, which leads to the sorting of heavy minerals from the light minerals and thus concentrates the selected heavy minerals rather than overall homogenized sediments in that region. Thus, the impact of the sorting effect also was determined based on the selective metals and their ratios in the present study. In Al₂O₃-TiO₂-Zr plot (Garcia et al., 1994) shown in Fig. 5, all the samples are enriched with either TiO₂ or Zr and lesser concentrations of Al₂O₃, which confirms that TiO2 and Zr are mainly controlled by Ti-bearing minerals (Ilmenite, rutile/anatase) and zircon respectively due to the influence of sorting on the beaches and enrichment of high compositional maturity. This has been further supported by the XRD (Table 2) analysis that the IRS sediments are concentrated with ilmenite, zircon and rutile while QRS sediments are enriched with quartz, garnet and spinel.

In summary, based on the indices calculated, the IRS are preferentially contaminated by the metals namely, W, Th, Nb, U, and Pb while the QRS are preferentially contaminated by W, Th, Pb, Nb, Cu and Co. The enrichments of these metals in these sediments are mainly of natural origin and these metals are associated with the minerals' lattice rather than in the exchangeable fraction and thus have less mobility, which has been clearly supported by the mineralogy. The sediments of the IRS group show the presence of quartz, ilmenite, sillimanite, zircon, garnet and rutile/anatase due to the sorting effect by the beach action while QRS sediments are composed of quartz, calcite, garnet, pyroxenes and spinel. The PLI values for IRS are in the ranges of 2.11 to 8.13 (avg: 5.10), which

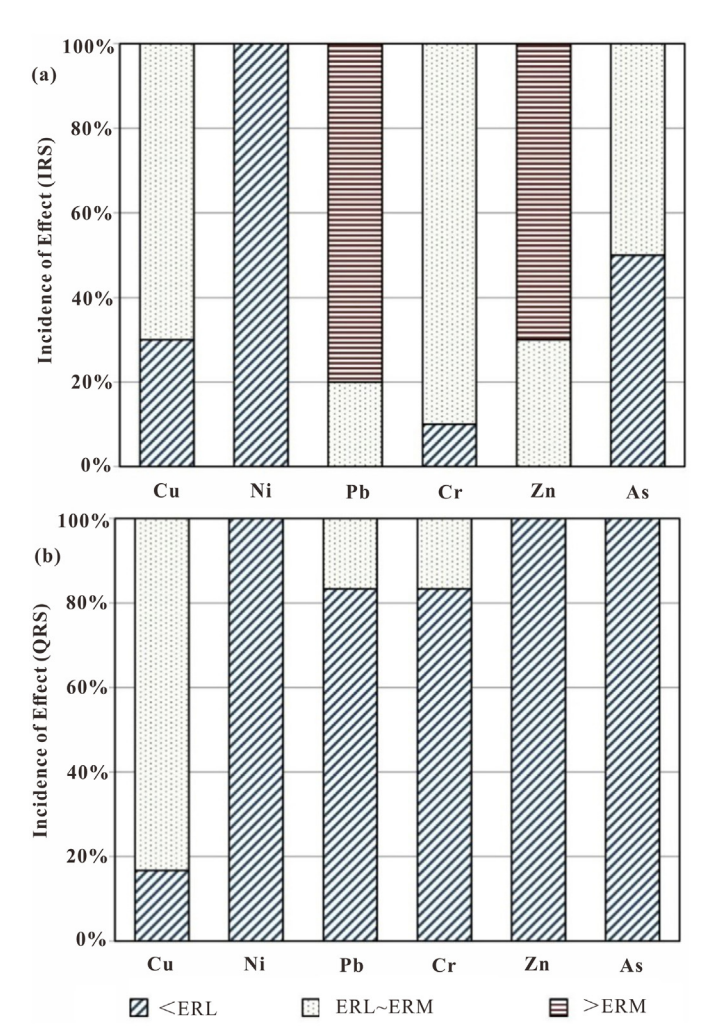


Fig. 6. Biological effects of selected metals on living organisms based on ERL and ERM values (a) IRS and (b) QRS.

indicate a moderate to highly polluted nature. The QRS shows PLI values between 0.72 and 2.00 (avg: 1.12), which indicates unpolluted to moderately polluted nature. For both groups of sediments, the high PLI values are controlled by W followed by Th, Nb and Pb.

5.3. Ecological risk assessment and the biological effect

As per average ER values in IRS, the Cr and Zn fall under low risk with values of 3.94 and 7.33; Cu with a value of 57.88 falls under moderate risk; As and Pb fall under considerable risk with values of 83.26 and 92.67. In QRS, the ER for Cr, As, Zn and Pb fall under the low-risk category with values of 0.93, 6.57, 0.90 and 13.69 respectively. The ER value of Cu is comparatively higher (104.11) and shows a considerable risk. Similarly, the average RI value in the IRS (245.09) and QRS (126.20) represents a moderate risk respectively.

Zn and Pb show higher than ERM values in IRS (Fig. 6a), and will have possible detrimental effects by these metals in the 70% and 80% of stations respectively. Similarly, the ilmenite-rich sediments (IRS) have recorded Cr, Cu, As, Zn and Pb concentrations in the ranges between ERL and ERM with the effect of 90%, 70%, 50%, 30%, and 20% respectively. Ni shows less than ERL and has no effect in all the IRS stations. In QRS (Fig. 6b), none of the metals exceeded the ERM values but only Cu, Pb and Cr have the effect of 83.33%, 16.67% and 16.67% of stations by having their concentrations in the range between ERL and ERM values. No effect is exhibited by the

Ni, Zn and As for all the stations; Pb and Cr for 83.33% of stations; and Cu for 16.67% of stations.

The study reveals that Thiruvananthapuram coastal beach sediments are notably polluted, with IRS showing high concentrations of W and Th and QRS indicating pollution from W and Cu. The presence of significant contamination, particularly with Cu and Zn, highlights the importance of assessing bioavailability for accurate toxicity determinations and understanding potential transfers to ecosystems. The investigation of metal pollution in Thiruvananthapuram coastal region beach sediments employed various pollution indices, with differing results between IRS and QRS. Surface sediments primarily exhibited enrichment in W, Th, Nb, U, and Pb, while other heavy metals showed minor to moderate enrichment. Significant contamination was noted for Cu in both groups and Zn in QRS, with Fe in IRS and Nb in QRS also displaying considerable contamination. Overall, IRS was found to be moderate to highly polluted, particularly with high concentrations of W and Th, while QRS showed pollution primarily from W and Cu, with the absence of U. The accumulation of elements with varying toxic potentials in sediments, influenced by geogenic and anthropogenic processes, underscores the need for further assessment of bioavailability to determine actual toxicity and potential transfer to ecosystems. Though many metals show high enrichments and potential environmental impacts, their concentrations are mainly controlled by the various heavy minerals, which are accumulated in the beach due to the sorting effects and beach dynamics. In summary, the study highlights concerns about specific pollutants, their concentrations, and the potential environmental impacts, emphasizing the importance of further research and proactive measures to address these issues. Also, the state government when implementing the Responsible Tourism policy, the necessary actions will be taken for the promotion of sustainable tourism in the state.

6. Conclusion and policy recommendation

The metal pollution from the beach sediments of Thiruvananthapuram coastal region was investigated based on several pollution indices. The IRS and QRS yielded the results differently and metal concentrations are mainly controlled by the selected heavy and light minerals. The role of Fe-Mn oxides and sulphides/organics is lesser, however, needs further study to confirm the association of metals in these fractions. Though the trends of the average indices values are different, W, Th and U are enriched in IRS, which is highly contaminated by these metals while QRS are enriched/contaminated by W and Th. For IRS, W, Th, Nb and U are highly contaminated as per CF; Igeo shows maximum values for W and Th; maximum EF is shown by W, Th, Nb and U; Zn and Pb are mostly in the >ERM range; and PLI shows that the IRS are moderate to highly polluted. Overall, IRS is contaminated with high-value ranges of W and Th. Pb and As show considerable risk as per ER. RI shows that this group as moderate risk. In QRS, W and Cu are majorly contaminated as per CF; W only shows huge value as per Igeo and EF; majorly Cu falls within the range of ERL and ERM whereas others mostly range under ERL; and PLI shows that this group is unpolluted to moderately polluted. These metals are mainly controlled by the heavy and light minerals and these minerals are mainly accumulated and controlled by the sorting effect in the beach. The higher concentration of these heavy minerals has the economic potential for mining, however, may have high radioactivity in the studied tourist beaches (i.e., IRS), which needs to be further assessed. Together, it can be construed that though there are certain elements, albeit at differential toxic potentials are accumulating in the sediments, perhaps under the combined influences of geogenic and anthropogenic processes, their bioavailability needs to be ascertained for succinct determinations of actual toxicity and their potential transfer to the biotic and other systems. Since we did not conduct either career phases and sequential extraction analysis, the mobility and bioavailability are not able to be addressed, which is the limitation of the present study. This will be addressed soon in future research. In addition, Kerala state has drafted a Responsible Tourism policy and this has three kinds of responsibilities, which are social, economic and environmental. This research outcome will contribute towards the baseline for any initiatives planned for the benefit of the local communities and tourism development. Upon launching of the responsible tourism policy in the Kerala state, all the beaches will be periodically assessed in terms of social, economic and environmental aspects, which will ensure environmental sustainability and promote sustainable tourism.

Declaration of Competing Interest

The authors declare that they have no known competing financial interests or personal relationships that could have appeared to influence the work reported in this paper.

CRediT authorship contribution statement

Mu. Ramkumar: Conceptualization, Data curation, Formal analysis, Validation, Writing – original draft, Writing – review & editing. R. Nagarajan: Data curation, Writing – review & editing. P. Athira: Data curation, Formal analysis, Validation. Anupam Sharma: Formal analysis, Writing – review & editing. P. Gopika: Resources, Formal analysis. AL Fathima: Validation, Writing – review & editing. A. Manobalaji: Validation, Writing – review & editing. R. Mohanraj: Writing – review & editing.

Acknowledgments

The Memorandum of Understanding signed between the Periyar University and the Curtin University Sarawak, Malaysia has helped initiate collaborative research work between the authors for which MR and RN thank their respective institutions. The approval of research collaboration between the Periyar University and Birbal Sahni Institute of Paleosciences was made by the RAC of BSIP for which MR and AS express their thankfulness.

Supplementary materials

Supplementary material associated with this article can be found, in the online version, at doi:10.1016/j.geogeo.2023.100244.

References

Abbasi, A., Heshm, M.H.Z., Alotaibi, B.M., 2023. Radioactivity concentration and radiological risk assessment of beach sand along the coastline in the Mediterranean Sea. Mar. Pollut. Bull. doi:10.1016/j.marpolbul.2023.115527.

Aide, M.T., Aide, C., 2012. Rare Earth elements: their importance in understanding soil genesis. ISRN Soil Sci. 1–11. doi:10.5402/2012/783876, 2012.

Anandkumar, A., Li, J., Prabakaran, K., Jia, ZXi, Leng, Z., Nagarajan, R., Du, D., 2020. Accumulation of toxic elements in an invasive crayfish species (Procambarus clarkii) and its health risk assessment to humans. J. Food Compos. Anal. 88, 103449. doi:10.1016/j.jfca.2020.103449.

Anandkumar, A., Nagarajan, R., Sellappa Gounder, E., Prabakaran, K., 2022. Seasonal variation and mobility of trace metals in the beach sediments of NW Borneo. Chemosphere 287, 132069. doi:10.1016/j.chemosphere.2021.132069.

Anandkumar, A., Vijith, H., Nagarajan, R., Jonathan, M.P., 2019. Evaluation of decadal shoreline changes in the Coastal Region of Miri, Sarawak, Malaysia (Chapter 7) In: Krishnamurthy, R.R., Jonathan, M.P., Srinivasalu, S. Glaeser, B. (Eds) Coastal Management: Global Challenges and Innovations, Elsevier, Amsterdam., pp. 95–119. doi:10.1016/B978-0-12-810473-6.00008-X.

Angulo, E., 1996. The tomlinson pollution load index applied to heavy metal, 'Mussel-Watch' data: a useful index to assess coastal pollution. Sci. Total Environ. 187 (1), 19–56. doi:10.1016/0048-9697(96)05128-5.

Anshuman, M., Prasanna, M.V., Nagarajan, R., Chidambaram, S., 2023. Spatiotem-poral distribution of microplastics in Miri coastal area, NW Borneo: inference from a periodical observation. Environ. Sci. Pollut. Res. 30, 103225–103243. doi:10.1007/s11356-023-29582-7.

- Bray, L., Faulwetter, S., Kaberi, H., Karageorgis, A.P., Kastanidi, E., Katsiaras, N., Pavlidou, A., Providakis, N., Sigala, K., Voutsinas, E., Zeri, C., 2022. Assessing pressure drivers on the benthic ecosystem in the coastal zone of Western Messinia, Greece. Estuar. Coast. Shelf Sci. 274, 107935. doi:10.1016/j.ecss.2022.107935.
- Buccolieri, A., Buccolieri, G., Cardellicchio, N., Dell'Atti, A., Di Leo, A., Maci, A., 2006. Heavy metals in marine sediments of Taranto Gulf (Ionian Sea, Southern Italy). Mar. Chem. 99 (1–4), 227–235. doi:10.1016/j.marchem.2005.09.009.
- Buzzi, N.S., Menéndez, M.C., Truchet, D.M., Delgado, A.L., Severini, M.D.F., 2022. An overview on metal pollution on touristic sandy beaches: is the COVID-19 pandemic an opportunity to improve coastal management? Mar. Pollut. Bull. 174, 113275. doi:10.1016/j.marpollbul.2021.113275.
- Chen, C.W., Kao, C.M., Chen, C.F., Dong, C.D., 2007. Distribution and accumulation of heavy metals in the sediments of Kaohsiung Harbor, Taiwan. Chemosphere 66 (8), 1431–1440. doi:10.1016/j.chemosphere.2006.09.030.
- Dessai, A.G., 2023. Sustainable tourism. In: Environment, Resources and Sustainable Tourism: Goa as a Case Study. Springer Nature Singapore, pp. 187–228. Djumanto, M.E.L., Lazuardi, M.E., Zainudin, I.M., Ridarwati, S., 2022. The role of
- Djumanto, M.E.L., Lazuardi, M.E., Zainudin, I.M., Ridarwati, S., 2022. The role of marine-protected areas as a life support for fishery communities: Indonesian perspective. IntechOpen 93. doi:10.5772/intechopen.100214.
- Dodge-Wan, D., Nagarajan, R., 2019. Typology and mechanisms of coastal erosion in siliciclastic rocks of the NW Borneo coastline (Sarawak, Malaysia): a field approach. In Ramkumar, Mu. Arthur James, R., Menier, D., Kumaraswamy K., (Eds.). Coastal Zone Management: Global Perspectives, Regional Processes, Local Issues. Elsevier, Amsterdam, pp.65–98. doi: 10.1016/B978-0-12-814350-6.00003-3.
- Evelpidou, N., Tzouxanioti, M., Liaskos, A., 2022. Coastal erosion: the future of sandy beaches. Proc. Eur. Acad. Sci. Arts 1, 1–16.
- Feng, H., Han, X., Zhang, W., Yu, L., 2004. A preliminary study of heavy metal contamination in Yangtze River intertidal zone due to urbanization. Mar. Pollut. Bull. 49 (11–12), 910–915. doi:10.1016/j.marpolbul.2004.06.014.
- Francois, G., Katrin, E., Elke, F., Chantal, G., 2011. Marine Pollution: Let us not forget beach sand. Environ. Sci. Eur. doi:10.1186/2190-4715-23-40.
- Garcia, D., Fonteilles, M., Moutte, J., 1994. Sedimentary fractionations between Al, Ti, and Zr and the genesis of strongly peraluminous granites. J. Geol. 102 (4), 411–422. doi:10.1086/629683.
- Garzon, J.L., Ferreira, Ó., Plomaritis, T.A., 2022. Modeling of coastal erosion in exposed and groin-protected steep beaches. J. Waterw. Port Coast. Ocean Eng. 148 (6), 04022018.
- Gayathri, V., Muralisankar, T., Rajaram, R., Muniasamy, M., Santhanam, P., 2020. Assessment of heavy metals pollution in noyyal and Chinnar Rivers, Western Ghats of Tamil Nadu, India with reference to crabs (Gecarcinucidae)—A baseline study. Bull. Environ. Contam. Toxicol. 105, 538–545. doi:10.1007/s00128-020-02986-8.
- Ghosh, P. K., Datta, D., 2012. Coastal tourism and beach sustainability- An assessment of community perceptions in Kovalam, India. Malaysia J. Soc. Space 8 (7), 75–87
- Godwyn-Paulson, P., Jonathan, M.P., Rodríguez-Espinosa, P.F., Rodríguez-Figueroa, G.M., 2022. Rare earth element enrichments in beach sediments from Santa Rosalia mining region, Mexico: an index-based environmental approach. Mar. Pollut. Bull. 174, 113271.
- Gunes, G., 2022. The change of metal pollution in the water and sediment of the Bartin Riverin rainy and dry seasons. Environ. Eng. Res. 27 (2), 200701. doi:10. 4491/EER.2020.701.
- Hailu, F.F., Bitew, W.T., Ayele, T.G., Zawka, S.D., 2023. Marine protected areas for resilience and economic development. Aquat. Living Resour. 36, 22. doi:10.1051/alr/2023016.
- Hakanson, L., 1980. An ecological risk index for aquatic pollution control.a sedimentological approach. Water Res. 14 (8), 975–1001. doi:10.1016/0043-1354(80) 90143-8.
- Harikumar, P.S., Jisha, T.S., 2010. Distribution pattern of trace metal pollutants in the sediments of an urban wetland in the Southwest Coast of India. Int. J. Eng. Sci. Technol. 2, 840–850.
- Harmesa, H., Lestari, L., Budiyanto, F., Purbonegoro, T., Wahyudi, A.A.J., 2023. Preliminary study of geochemical speciation of copper and nickel in coastal sediments in Surabaya, Indonesia. Environ. Sci. Pollut. Res. 1–18.
- Ho, H.H., Swennen, R., Cappuyns, V., Vassilieva, E., Van Tran, T., 2012. Necessity of normalization to aluminum to assess the contamination by heavy metals and arsenic in sediments near Haiphong Harbor, Vietnam. J. Asian Earth Sci. 56, 229-239. doi:10.1016/jijseaes.2012.05.015.
- Hossain, M.B., Shanta, T.B., Ahmed, A.S.S., Hossain, M.K., Semme, S.A., 2019. Baseline study of heavy metal contamination in the Sangu River estuary, Chattogram, Bangladesh. Mar. Pollut. Bull. 140, 255–261. doi:10.1016/j.marpolbul.2019.01.058.
- Hossain, M.S., Rahman, A., Shahriar, M.S., Bari, Z., Yasir, M., 2023a. REEs enriched heavy minerals from the river and beach sands of Bangladesh. Arab. J. Geosci. 16 (1), 91.
- Hossain, M.S., Yasir, M., Shahriar, M.S., Jahan, M., Liu, S., Niang, A.J., 2023b. Morphological change assessment of a coastal island in SE Bangladesh reveal high accumulation rates. Reg. Stud. Mar. Sci. 62, 102969.
- Hui, P.X., Nagarajan, R., Ramkumar, M., Ng, T.F., Taib, N.I., Mathew, M.J., Sautter, B., Siddiqui, N.A., Poppelreiter, M.C., 2022. Geochemical evolution of structure-bedding controlled hydrothermal dolomites of the Kinta Valley, Western Malaysia. Carbonates Evaporites 37, 62. doi:10.1007/s13146-022-00802-4.
- Irrgang, A.M., Bendixen, M., Farquharson, L.M., Baranskaya, A.V., Erikson, L.H., Gibbs, A.E., Ogorodov, S.A., Overduin, P.P., Lantuit, H., Grigoriev, M.N., Jones, B.M., 2022. Drivers, dynamics and impacts of changing Arctic coasts. Nat. Rev. Earth Environ. 3 (1), 39–54.

- Isangedighi, I.A., David, G.S., 2019. Heavy metals contamination in fish: effects on human health. J. Aquat. Sci. Mar. Biol. 2 (4), 7–12.
- Jayaprakash, M., Nagarajan, R., Velmurugan, P.M., Sathiyamoorthy, J., Krishnamurthy, R.R., Urban, B., 2012. Assessment of trace metal contamination in a historical freshwater canal (Buckingham Canal), Chennai, India. Environ. Monit. Assess. 184 (12), 7407–7424. doi:10.1007/s10661-011-2509-5.
- Jéssica, V., Ana, A., Lourenco, R., Bernado, D., Maira, P., 2021. Baseline study of trace element concentrations in sediments of the intertidal zone of Amazonian Oceanic Beaches. Front. Mar. Sci. doi:10.3389/fmars.2021.671390.
- Kaviarasan, T., Dhineka, K., Sambandam, M., Sivadas, S.K., Sivyer, D., Hoehn, D., Pradhan, U., Mishra, P., Murthy, M.R., 2022. Impact of multiple beach activities on litter and microplastic composition, distribution, and characterization along the southeast coast of India. Ocean Coast Manag. 223, 106177. doi:10.1016/j. ocecoaman.2022.106177.
- Khuu, D.T., Jones, P.J., Ekins, P., 2023. Development of Marine Protected Areas (MPAs) in Vietnam from a coevolutionary governance perspective: challenges of unholy alliances between the state, businesses and NGOs. Environ. Sci. Policy 149, 103560. doi:10.1016/j.envsci.2023.103560.
- Kumar, S.B., Padhi, R.K., Mohanty, A.K., Satpathy, K.K., 2017. Elemental distribution and trace metal contamination in the surface sediment of south east coast of India. Mar. Pollut. Bull. 114 (2), 1164–1170. doi:10.1016/j.marpolbul.2016.10.038.
- Long, E.R., Ingersoll, C.G., MacDonald, D.D., 2006. Calculation and uses of mean sediment quality guideline quotients: a critical review. Environ. Sci. Technol. 40 (6), 1726–1736. doi:10.1021/es058012d.
- Long, E.R., MacDonald, D.D., Smith, S.L., Calder, F.D., 1995. Incidence of adverse biological effects within ranges of chemical concentrations in marine and estuarine sediments. Environ. Manag. 19, 81–97. doi:10.1007/bf02472006.
- Lozano, R., Bernal, J.P., 2005. Characterization of a new set of eight geochemical reference materials for XRF major and trace element analysis. Rev. Mex. Cienc. Geol. 22, 329–344.
- Mahmoud, A., Ahmed, M.E., El Azab, A., Alfi, S.M., Hani, H.A., Hanfi, M.Y.M., 2022. Radioactive risk assessment of beach sand along the coastline of mediterranean sea at El-Arish area,North Sinai, Egypt. Mar. Pollut. Bull. 177. doi:10.1016/j.marpolbul.2022.113494
- McLennan, S.M., 2001. Relationships between the trace element composition of sedimentary rocks and upper continental crust. Geochem. Geophys. Geosyst. 2 (4). doi:10.1029/2000 gc000109.
- Mohanty, S., Adikaram, M., Sengupta, D., Madhubashini, N., Wijesiri, C., Adak, S., Bera, B., 2023. Geochemical, mineralogical and textural nature of beach placers, north-east Sri Lanka: implications for provenance and potential resource. Int. J. Sediment. Res. 38 (2), 279–293. doi:10.1016/j.ijsrc.2022.09.004.
- Moodley, R., Mahlangeni, N.T., Reddy, P., 2021. Determination of heavy metals in selected fish species and seawater from the South Durban Industrial Basin, KwaZulu-Natal, South Africa. Environ. Monit. Assess. 193, 206. doi:10.1007/ s10661-021-09014-0.
- Mugoša, B., Đurović, D., Nedović-Vuković, M., Barjaktarović-Labović, S., Vrvić, M., 2016. Assessment of ecological risk of heavy metal contamination in coastal municipalities of Montenegro. Int. J. Environ. Res. Public Health 13 (4), 393. doi:10.3390/ijerph13040393.
- Müller, G., 1969. Index of geoaccumulation in sediments of the Rhine River. Geo-Journal 2, 108-118.
- Müller, G., 1981. The heavy metal pollution of the sediments of neckars and its tributary: a stocktaking. Chem. Ztg. 105, 157–164.
- Nagarajan, R., Anandkumar, A., Hussain, S.M., Jonathan, M.P., Ramkumar, Mu., Eswaramoorthi, S., Saptoro, A., Chua, H.B., 2019. Geochemical characterization of beach sediments of the NW Borneo, SE Asia: implications on provenance, weathering intensity and assessment of coastal environmental status. In: Coastal Zone Management: Global Perspectives, Regional Processes, Local Issues. Elsevier, pp. 279–330. doi:10.1016/B978-0-12-814350-6.00012-4.
- Nagarajan, R., Eswaramoorthi, S., Anandkumar, A., Ramkumar, M., 2023. Geochemical fractionation, mobility of elements and environmental significance of surface sediments in a Tropical River, Borneo. Mar. Pollut. Bull. 192, 115090. doi:10.1016/j.marpolbul.2023.115090.
- Pekey, H., 2006. Heavy metal pollution assessment in sediments of the Izmit Bay, Turkey. Environ. Monit. Assess. 123, 219–231. doi:10.1007/s10661-006-9192-y.
- Pradeep, J., Shaji, E., Chandran, C.S.S., H, A., Chandra, S.S.V., Dev, S.G.D., Babu, D.S.S, 2022. Assessment of coastal variations due to climate change using remote sensing and machine learning techniques: a case study from west coast of India. Estuar. Coast. Shelf Sci. 275, 107968. doi:10.1016/j.ecss.2022.107968
- Qiao, Y., Yang, Y., Gu, J., Zhao, J., 2013. Distribution and geochemical speciation of heavy metals in sediments from coastal area suffered rapid urbanization, a case study of Shantou Bay, China. Mar. Pollut. Bull. 68 (1–2), 140–146. doi:10.1016/j. marpolbul.2012.12.003.
- Rahimi, A., Adabi, M.H., Aghanabati, A., Majidifard, M.R., Jamali, A.M., 2016. Dolomitization mechanism based on petrography and geochemistry in the shotori formation (Middle Triassic), Central Iran. Open J. Geol. 6, 1149–1168. doi:10.4236/
- Ramesh, M., Sheela Nair, L., Amrutha Raj, V., Sarankumar, S.G., Akhildev, S., Arya, R.P., 2023. Advanced remote sensing methods for high-resolution, costeffective monitoring of the coastal morphology using video beach monitoring system (VBMS), CoastSnap, and CoastSat techniques. In: Coasts, Estuaries and Lakes: Implications for Sustainable Development. Springer International Publishing, Cham, pp. 427–444.

- Ramkumar, M., Sudha Rani, P., Gandhi, M.S., Pattabhi Ramayya, M., Rajani Kumari, V., Bhagavan, K.V.S., Swamy, A.S.R., 2000. Textural characteristics and depositional sedimentary environments of the Modern Godavari Delta. J. Geol. Soc. India 56. 471–487.
- Ramkumar, Mu., Stüben, D., Berner, Z., 2006. Elemental interrelationships and depositional controls of barremian-danian strata of the Cauvery Basin, South India. Indian J. Geochem. 21 (2), 341–367.
- Rejith, R.G., Sundararajan, M., Peer Mohamed, A., Satyanarayanan, M., 2021. Raman-XPS spectroscopy, REE chemistry, and surface morphology of Fe-Ti oxide heavy mineral sands: a case study from Varkala-Kovalam coast, South-West India. Appl. Earth Sci. 130 (3), 161–173. doi:10.1080/25726838.2021.1911584.
- Rejith, R.G., Sundararajan, M., Ramaswamy, S., Peer Mohamed, A.A., Satyanarayanan, M., 2022. Physico-chemical characterization of detrital sillimanite and garnet: insights into REE elements, crystal structure and morphology. Mar. Georesources Geotechnol. doi:10.1080/1064119x.2022.2137713.
- Saengsupavanich, C., Pranzini, E., Ariffin, E.H., Yun, L.S., 2023. Jeopardizing the environment with beach nourishment. Sci. Total Environ. 868, 161485. doi:10.1016/j.scitotenv.2023.161485.
- Santos, E.E., Lauria, D.C., Porto da Silveira, C.L., 2004. Assessment of daily intake of trace elements due to consumption of foodstuffs by adult inhabitants of Rio de Janeiro City. Sci. Total Environ. 327 (1–3), 69–79. doi:10.1016/j.scitotenv.2004.01. 016.
- Selvaraj, K., Ram Mohan, V., Szefer, P., 2004. Evaluation of metal contamination in coastal sediments of the Bay of Bengal, India: geochemical and statistical approaches. Mar. Pollut. Bull. 49 (3), 174–185. doi:10.1016/j.marpolbul.2004.02. 006.
- Sheela, A.M., Letha, J., Joseph, S., Thomas, J., 2012. Assessment of heavy metal contamination in coastal lake sediments associated with urbanization: southern Kerala, India. Lakes Reserv. Sci. Policy Manag. Sustain. Use 17 (2), 97–112. doi:10.1111/j.1440-1770.2012.00501.x.

- Suresh, G., Ramasamy, V., Sundarrajan, M., Paramasivam, K., 2015. Spatial and vertical distributions of heavy metals and their potential toxicity levels in various beach sediments from high-background-radiation area, Kerala, India. Mar. Pollut. Bull. 91 (1), 389–400. doi:10.1016/j.marpolbul.2014.
- Tomlinson, D.L., Wilson, J.G., Harris, C.R., Jeffrey, D.W., 1980. Problems in the assessment of heavy-metal levels in estuaries and the formation of a pollution index. Helgol. Meeresunters. 33, 566–575. doi:10.1007/bf02414780.
- Venkatramanan, S., Chung, S.Y., Selvam, S., Sivakumar, K., Soundhariya, G.R., Elzain, H.E., Bhuyan, M.S., 2022. Characteristics of microplastics in the beach sediments of Marina tourist beach, Chennai, India. Mar. Pollut. Bull. 176, 113409. doi:10.1016/i.marpolbul.2022.113409.
- Vineethkumar, V., Sayooj, V.V., Shimod, K.P., Prakash, V., 2020. Estimation of pollution indices and hazard evaluation from trace elements concentration in coastal sediments of Kerala, Southwest Coast of India. Bull. Natl. Res. Cent. 44, 198. doi:10.1186/s42269-020-00455-0.
- Wang, W., Wu, F., Yin, T., Jiang, S., Tang, S., 2023. Distribution, source, and contamination assessment of heavy metals in surface sediments of the Zhifu Bay in Northern China. Mar. Pollut. Bull. 194, 115449. doi:10.1016/j.marpolbul.2023. 115449
- Zhong, W., Zhang, Y., Wu, Z., Yang, R., Chen, X., Yang, J., Zhu, L., 2018. Health risk assessment of heavy metals in freshwater fish in the central and eastern North China. Ecotoxicol. Environ. Saf. 157, 343–349. doi:10.1016/j.ecoenv.2018. 03.048.
- Zoller, W.H., Gladney, E.S., Duce, R.A., 1974. Atmospheric concentrations and sources of trace metals at the South Pole. Science 183, 198–200. doi:10.1126/science.183. 4121198